Front. Chem. Sci. Eng. 2021, 15(4): 954–959
https://doi.org/10.1007/s11705-020-2028-4

RESEARCH ARTICLE

Effect of sodium bicarbonate solution on methyltrimethoxysilane-derived silica aerogels dried at ambient pressure

Yujing Liu (✉)[1], Xiao Han[1], Balati Kuerbanjiang[2*], Vlado K. Lazarov[2], Lidija Šiller (✉)[1]

1 School of Engineering, Newcastle University, Newcastle upon Tyne NE1 7RU, UK
2 Department of Physics, University of York, York YO10 5DD, UK

Abstract Here we present an economical ambient pressure drying method of preparing monolithic silica aerogels from methyltrimethoxysilane precursor while using sodium bicarbonate solution as the exchanging solvent. We prepared silica aerogels with a density and a specific surface area of 0.053 $g \cdot cm^{-3}$ and 423 $m^2 \cdot g^{-1}$, respectively. The average pore diameter of silica aerogels is 23 nm as the pore specific volume is 1.11 $cm^3 \cdot g^{-1}$. Further, the contact angle between water droplet and the surface of silica aerogels in specific condition can be as high as 166°, which indicates a super-hydrophobic surface of aerogels.

Keywords silica aerogel, methyltrimethoxysilane, solvent exchange, sodium bicarbonate, trimethylchlorosilane, ambient pressure drying

1 Introduction

Silica aerogels (SAs) are highly porous nanomaterials with extremely low densities, high specific surface areas and high porosities [1]. Due to these properties, SAs have various potential applications, e.g., drug delivery systems [2], energy storage systems [3], cosmic dust capture [4], paints [5], food packaging [6], and insulation in buildings [7]. Despite the advantages of SAs, there are still some practical limitations. For example, supercritical drying, freeze drying and ambient pressure drying (APD) methods are commonly used in the manufacturing process of SAs during the drying stage. However, the most conventional supercritical drying method requires expensive equipment with high-pressure operational conditions [8,9]. Freeze drying method applies sublimation of pore liquid but may break the network of aerogel [10]. The less energy-intensive alternative is APD method, which usually relies on low surface tension solvents, e.g., hexane, heptane, xylene, etc. [11]. Thus, this is still uneconomical because of large quantities of organic low surface tension solvents used in scaling up SAs production in APD method. However recently, it was suggested that a low-cost combination of sodium bicarbonate with trimethylchlorosilane (TMCS) due to *in-situ* generation of CO_2 can prevent wet gels from shrinkage and collapse in this APD method [12].

Furthermore, conventional SAs made from precursor tetraethoxysilane and tetramethoxysilane are usually moisture-sensitive because of the hydrophilic surface [9]. Studies of hydrophobic SAs prepared from methyltrimethoxysilane (MTMS) as the precursor, which has a methyl group '–CH_3' attached to 'Si–O' framework, generally focus on dilution of precursor [13,14], the concentration of catalyst [14,15], effect of surfactant [15,16]. To the best of our knowledge, there has been no report on using sodium bicarbonate solution as the exchanging solvent in APD method of MTMS-derived SAs, hence it is the aim of this study. In addition, we here present comparison in regard to properties of the MTMS-based SAs using deionized water, hexane and different concentration of sodium bicarbonate solutions during the APD process.

Received August 26, 2020; accepted October 17, 2020

E-mails: y.liu102@ncl.ac.uk (Liu Y), lidija.siller@ncl.ac.uk (Šiller L)

*Current address: Department of Physics, University of Oxford, Oxford OX1 3PU, UK

2 Experimental

2.1 Materials

All chemicals were used as received. MTMS (95%), oxalic acid powder (99%), sodium bicarbonate (99.5%), TMCS (98%) and hexane (95%) were purchased from Sigma-Aldrich. Ammonia solution (35% w/w), methanol (99.9%) and ethanol (99.8%) were purchased from Fisher Scientific.

2.2 Preparation

Wet gels were prepared via an acid-base catalysis sol-gel process [14]. Firstly, precursor MTMS, methanol and half of deionized water (in form of 0.01 $mol \cdot L^{-1}$ oxalic acid solution) were mixed in a 40 mL vial at a molar ratio of 1:32:8 while consistently stirring at 350 $r \cdot min^{-1}$ for 30 min. After 24 h, another half of water in form of 10 $mol \cdot L^{-1}$ ammonia solution was slowly dropped while stirring at 350 $r \cdot min^{-1}$ for 30 min. Gelation happened within 24 h, and then extra methanol was filled into the vial in case of shrinkage. This ageing process lasted 3 d, and 4 wet gels that are obtained were labelled as G1, G2, G3 and G4. At the solvent exchange stage, G1 was exchanged by deionized water, while G2 was first exchanged by ethanol and then by hexane. G3 and G4 were exchanged with 0.044 $g \cdot mL^{-1}$ and 0.022 $g \cdot mL^{-1}$ sodium bicarbonate solution, respectively. After full solvent exchange, G1 and G2 were dried at ambient pressure for 1 d. G3 and G4 were first poured with mixed solvent of TMCS and ethanol at volume ratio of 1:4, and then extra ethanol was filled into vials [12]. After washed by the mixed solvent of deionized water and ethanol at a volume ratio of 1:1, G3 and G4 were dried at ambient pressure for 1 d. Finally, four aerogel samples obtained were labelled as A1, A2, A3 and A4.

2.3 Characterisations

A Thermo-Scientific Surfer system was used to determine specific surface areas and pore size distributions in all samples. The specific surface area was found by measuring the adsorption-desorption isotherms at 77 K of gaseous N_2 using a Brunaer-Emmett-Teller analysis, while the pore size distributions were obtained from the same isotherms by the Barrett-Joyner-Halenda method.

The porosities of all samples were calculated by Eq. (1):

$$Porosity = \left(1 - \frac{\rho_{bulk}}{\rho_{skeletal}}\right) \times 100\%, \quad (1)$$

where ρ_{bulk} is determined by mass over volume. $\rho_{skeletal}$ is the skeletal density of MTMS-derived SAs, and it usually is 1.9 $g \cdot cm^{-3}$ [14].

X-ray diffraction (XRD) analysis was undertaken via a PANalytical X'Pert Pro multipurpose diffractometer by using Cu Kα X-rays. Samples were mounted on a low-background silicon substrate and diffraction scans covered a 2θ range of 5° to 90°. Fourier-transform infrared (FT-IR) spectroscopy, an IRAffinity-1s (Shimadzu Scientific Instruments), was used to study chemical bonds of SAs in the range of 500 to 4000 cm^{-1}, taken after 1-hour heating of samples at 120 °C in the oven in order to remove moisture. Furthermore, an angle meter CAM100 (KSV Instrument Ltd.) was used to measure the contact angle between deionized water droplet and surface of SAs. After coated with gold, microstructure morphology of SAs was measured with a scanning electron microscopy (SEM) (JEOL 7800F Prime). Transmission electron microscopy (TEM) experiments were carried out by a HT7800 (Hitachi High-Technologies Corporation) at Newcastle University after ultrasonication of SAs in ethanol until solution was dropped on the copper grid.

3 Results and discussion

Figure 1 presents the observation of all samples. We see that in Fig. 1(a) SAs are powder after solvent exchange step with deionized water while in Fig. 1(b) SAs in solvent exchange step with hexane and in Figs. 1(c,d) different concentration of sodium bicarbonate solution remain monolithic after the APD. Drying process causes more shrinkage of wet gels when solvent exchange was with hexane than sodium bicarbonate solution. This can be explained from previous work [12], which shows that SAs could stay monolithic because CO_2 produced from reaction between TMCS and sodium bicarbonate is trapped within the gels and stops collapse of porous structure of SAs. Also, wet gels exchanged with 0.044 $g \cdot mL^{-1}$ sodium bicarbonate solution (Fig. 1(c)) have less shrinkage than those with 0.022 $g \cdot mL^{-1}$ sodium bicarbonate solution (Fig. 1(d)) after APD process.

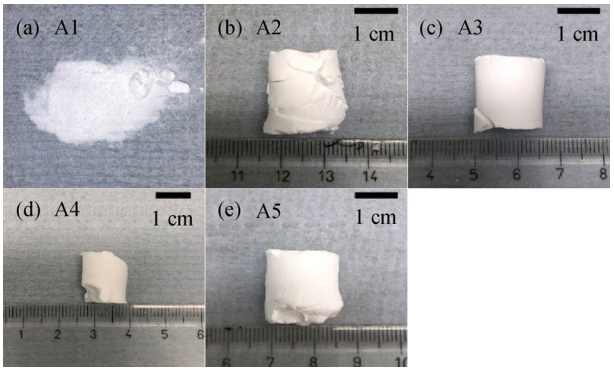

Fig. 1 MTMS-derived SAs via APD method while using (a) deionized water, (b) hexane, (c) 0.044 $g \cdot mL^{-1}$ sodium bicarbonate solution, (d) 0.022 $g \cdot mL^{-1}$ sodium bicarbonate solution in solvent exchange step, respectively along with (e) sample A3 after extra wash to remove salt, labelled as A5.

In general, XRD 2θ scans obtained from all SAs (Fig. 2) present a wider peak at 22° that is characteristic of amorphous silica [17]. The narrower peak at $2\theta < 10°$ has been observed in many previous studies with MTMS, tetraethoxysilane, PhTEOS, etc. precursors, see for example references [7,17–19]. It has been emphasised, that the origin of this peak is still controversial in literature, because peak has been assigned to the presence of fourfold siloxane rings or to a discrete structural unit in matrix based on an octametric silicon arrangement [19]. Additional recent hypothesis is that this peak at $2\theta < 10°$ is due to structure that consists of a siloxane network and organic layers containing ordered arrangements [19]. Peaks at 32°, 45°, 56°, 67° and 75° of sample A3 and A4 (see Figs. 2(c, d)) are corresponding to sodium chloride (NaCl) at (200), (220), (222), (400) and (420), respectively (PDF 00-005-0628). In addition, NaCl can be removed by extra wash with mixed solvent of deionized water and ethanol (Fig. 2(e)).

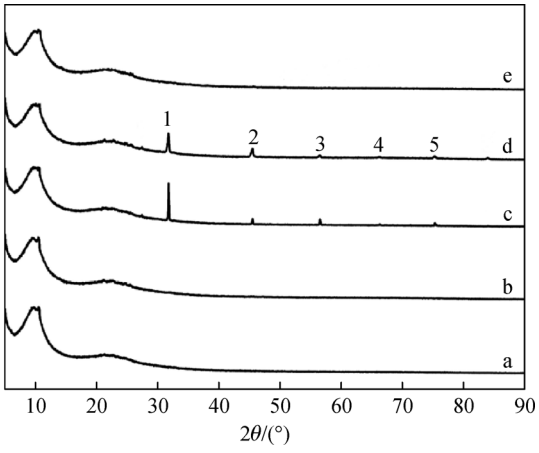

Fig. 2 XRD 2θ scans of MTMS-derived SAs using (a) deionized water, (b) hexane, (c) 0.044 $g \cdot mL^{-1}$ and (d) 0.022 $g \cdot mL^{-1}$ sodium bicarbonate solution in solvent exchange step, respectively. Peaks (1–5) appearing on patterns of c and d belong to NaCl (200), (220), (222), (400) and (420), which could be removed by extra wash with mixed solvent of ethanol and deionized water (e).

Physical properties of samples are presented in Table 1. Wet gels exchanged with sodium bicarbonate solution after APD process maintain the lower average pore diameter of 17 nm and pore specific volume of 0.53 $cm^3 \cdot g^{-1}$ whereas hexane offers sample a high specific surface area of 480 $cm^2 \cdot g^{-1}$. In addition, sodium bicarbonate provides SAs with the lowest bulk density of 0.053 $g \cdot cm^{-3}$. In other words, the porosity of samples using sodium bicarbonate solution in the solvent exchange step based on calculation was obtained as high as 97.2%. However, there are reductions on specific surface area and pore specific volume of SAs using sodium bicarbonate solution in solvent exchange step after extra wash of wet gels prior to drying.

Figure 3 shows the SEM micrographs of SAs synthesised with deionized water (a), hexane (b), 0.044 and 0.022 $g \cdot mL^{-1}$ sodium bicarbonate solution (c,d) in the solvent exchange step. All samples display a three-dimensional nanoporous structure. However, there is a visible coarsening of the structure with decreasing sodium bicarbonate concentration, reflecting in an increase in the average feature size observed in the micrographs together with a small porosity, which correlates well with the pore size increase for lower concentration of sodium bicarbo-

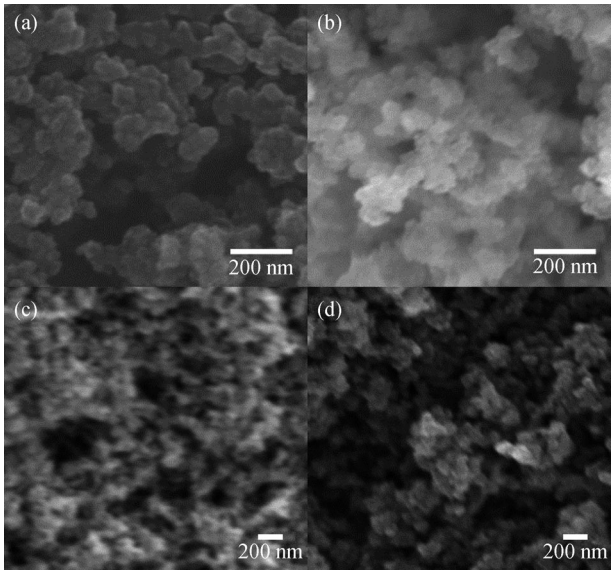

Fig. 3 SEM images of MTMS-derived SAs via APD method with the solvent exchange step with (a) deionized water, (b) hexane, (c) 0.044 $g \cdot mL^{-1}$ and (d) 0.022 $g \cdot mL^{-1}$ sodium bicarbonate solution, respectively.

Table 1 Physical properties of MTMS-derived SAs using deionized water (A1), hexane (A2), 0.044 $g \cdot mL^{-1}$ (A3) and 0.022 $g \cdot mL^{-1}$ sodium bicarbonate solution (A4) in solvent exchange step, respectively along with properties of sample A5 (A3 with extra wash prior to APD process)

Sample	A1	A2	A3	A4	A5
Specific surface area/($m^2 \cdot g^{-1}$)	422.7	480.6	423.6	406.4	313.3
Average diameter/nm	18.84	27.99	17.06	22.96	29.29
Pore specific volume/($cm^3 \cdot g^{-1}$)	0.57	0.76	1.11	0.53	0.87
Density/($g \cdot cm^{-3}$)	0.081	0.066	0.053	0.071	0.055
Porosity	95.7%	96.5%	97.2%	96.3%	97.1%

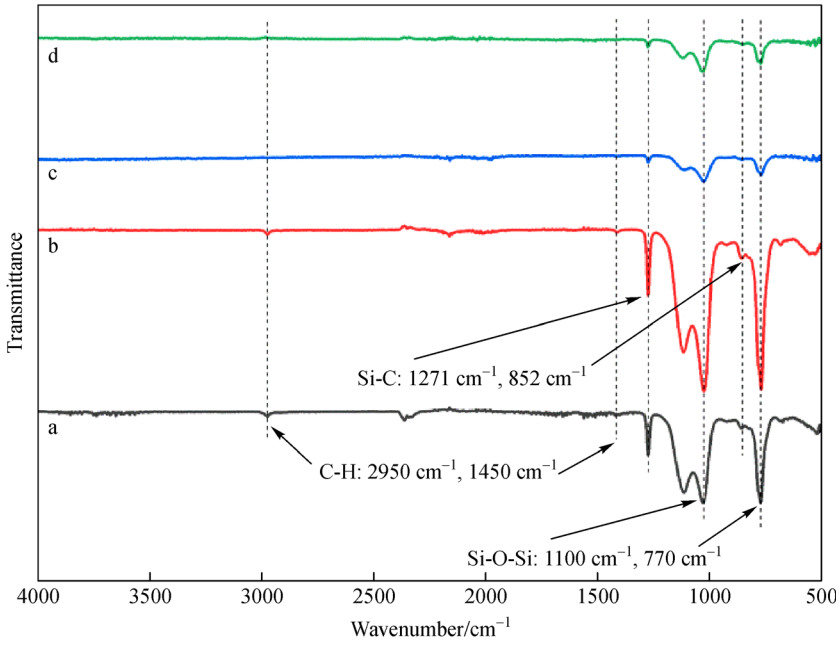

Fig. 4 FTIR spectra of MTMS-derived SAs using (a) deionized water, (b) hexane, (c) 0.044 g·mL^{-1} and (d) 0.022 g·mL^{-1} sodium bicarbonate solution in solvent exchange step, respectively.

nate with TMCS, which generates more CO_2 gas bubbles within a gel during pre-drying step, hence improving overall porosity as well as suppressing collapse of the holes, which then results in smaller pore size.

FTIR spectra of all SAs are presented in Fig. 4. It is noticeable that backbone of SAs 'Si-O-Si' is located at ~1100 cm^{-1} and 770 cm^{-1} which are asymmetric and symmetric modes, respectively [20]. Strong peaks at 1271 and 852 cm^{-1} correspond to 'Si-C' bond [21,22]. Peaks at 2950 and 1450 cm^{-1} are stretching and bending modes of 'C-H' bonding, respectively [20]. TEM images (Fig. 5) show the microstructure of the MTMS-derived aerogels. It is clearly that wet gels exchange with deionized water and hexane (Figs. 5(a,b)) after APD process have a more compact structure when compared to those exchanged with sodium bicarbonate solution (Figs. 5(c,d)). This is also correlated with reduced shrinkage of A3 and A4 samples observed in Fig. 1.

Investigation of hydrophobicity is shown in Fig. 6. We find that all samples are hydrophobic and float on water surface even after 15 d (see Figs. 6(a–c)). For further investigation of hydrophobicity, contact angle measurement between deionized water droplet and aerogels surface are presented in Figs. 6(d–g). The SAs using 0.022 g·mL^{-1} sodium bicarbonate solution in the solvent exchange step have the highest value of 166°, indicating a super-hydrophobicity [23]. Sample A3 using 0.044 g·mL^{-1} sodium bicarbonate solution has the lowest contact angle of 108°, which is likely due to the presence of residual NaCl that is by-product of reaction of sodium

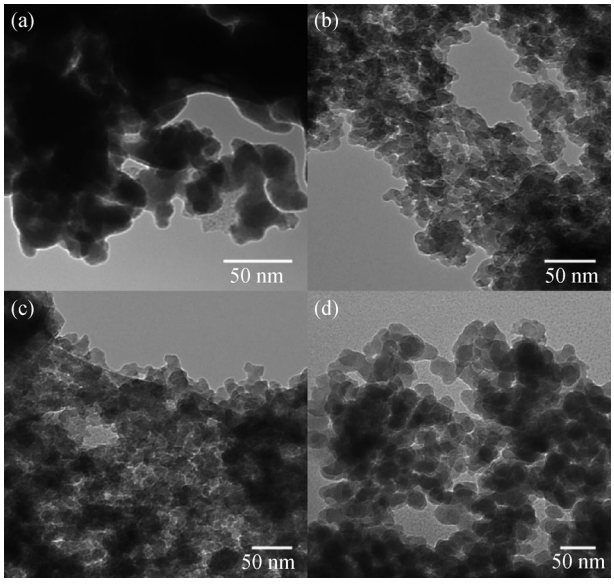

Fig. 5 TEM images of MTMS-derived SAs using in solvent exchange step (a) deionized water, (b) hexane, (c) 0.044 g·mL^{-1} and (d) 0.022 g·mL^{-1} sodium bicarbonate solution, respectively.

bicarbonate and TMCS. However, this contact angle increases to 141° after the A3 has been extra washed with mixed solvent of ethanol and deionized water (see Fig. 6(g)), NaCl has been removed from SAs (as confirmed by XRD in Fig. 2). The A2 sample, where solvent exchanged in wet gels with hexane, has a contact angle of 143°.

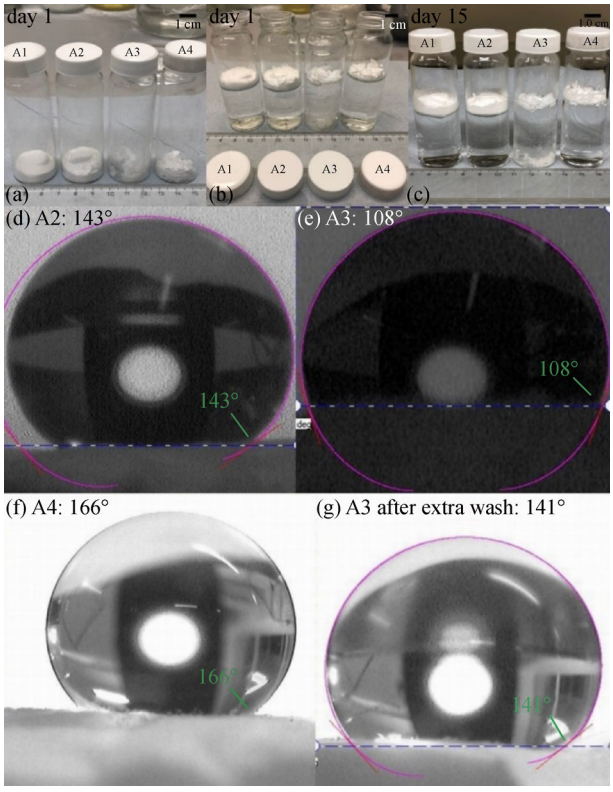

Fig. 6 Observations of hydrophobicity of (a–c) MTMS-derived SAs and (d–g) contact angle measurement of deionized water droplet and samples surface. A2, A3, A4 are MTMS-derived SAs using (d) hexane, (e) 0.044 $g \cdot mL^{-1}$ sodium bicarbonate solution and (f) 0.022 $g \cdot mL^{-1}$ sodium bicarbonate solution, respectively.

4 Conclusions

Super-hydrophobic SAs with the specific surface area of 423.6 $m^2 \cdot g^{-1}$, pore specific volume of 1.11 $cm^3 \cdot g^{-1}$, and density of 0.053 $g \cdot cm^{-3}$ were prepared from precursor MTMS via APD method by using sodium bicarbonate solution with TMCS in solvent exchange step. Comparing to deionized water, sodium bicarbonate solution prevents wet gels from collapse during APD process and reduces shrinkage of the wet gels due to generated CO_2 gas within the pores of those. Although high concentration of sodium bicarbonate solution improves porosity and reduces the shrinkage of the wet gels, it also increases the yield of by-product NaCl that requires extra washing step. This then still delivers SAs similar contact angle to samples using hexane in solvent exchange step. However, lower concentration sodium bicarbonate solution leads to super-hydrophobic SAs sample without any extra wash, with a contact angle as high as 166° , whereas hexane used SAs has a contact angle of 143° .

References

1. Hüsing N, Schubert U. Aerogels—airy materials: chemistry, structure, and properties. Angewandte Chemie International Edition, 1998, 37(1-2): 22–45
2. Wang C, Okubayashi S. 3D aerogel of cellulose triacetate with supercritical antisolvent process for drug delivery. Journal of Supercritical Fluids, 2019, 148: 33–41
3. Wang C, Liang W, Yang Y, Liu F, Sun H, Zhu Z, Li A. Biomass carbon aerogels based shape-stable phase change composites with high light-to-thermal efficiency for energy storage. Renewable Energy, 2020, 153: 182–192
4. Tsou P. Silica aerogel captures cosmic dust intact. Journal of Non-Crystalline Solids, 1995, 186: 415–427
5. Smirnova I, Gurikov P. Aerogels in chemical engineering: strategies toward tailor-made aerogels. Annual Review of Chemical and Biomolecular Engineering, 2017, 8(1): 307–334
6. da Silva F T, de Oliveira J P, Fonseca L M, Bruni G P, da Rosa Zavareze E, Dias A R G. Physically cross-linked aerogels based on germinated and non-germinated wheat starch and PEO for application as water absorbers for food packaging. International Journal of Biological Macromolecules, 2020, 155: 6–13
7. Ul Haq E, Zaidi S F A, Zubair M, Abdul Karim M R, Padmanabhan S K, Licciulli A. Hydrophobic silica aerogel glass-fibre composite with higher strength and thermal insulation based on methyltrimethoxysilane (MTMS) precursor. Energy and Building, 2017, 151: 494–500
8. Anderson A M, Carroll M K, Green E C, Melville J T, Bono M S. Hydrophobic silica aerogels prepared via rapid supercritical extraction. Journal of Sol-Gel Science and Technology, 2010, 53 (2): 199–207
9. Aegerter M A, Leventis N, Koebel M M. Aerogels Handbook. New York: Springer, 2011, 79, 105
10. Gurav J L, Jung I K, Park H H, Kang E S, Nadargi D Y. Silica aerogel: synthesis and applications. Journal of Nanomaterials, 2010, 2010: 409310
11. Rao A P, Rao A V, Pajonk G M. Hydrophobic and physical properties of the two step processed ambient pressure dried silica aerogels with various exchanging solvents. Journal of Sol-Gel Science and Technology, 2005, 36(3): 285–292
12. Han X, Hassan K T, Harvey A, Kulijer D, Oila A, Hunt M R C, Šiller L. Bioinspired synthesis of monolithic and layered aerogels. Advanced Materials, 2018, 30(23): 1706294
13. Bhagat S D, Oh C S, Kim Y H, Ahn Y S, Yeo J G. Methyltrimethoxysilane based monolithic silica aerogels via ambient pressure drying. Microporous and Mesoporous Materials, 2007, 100(1): 350–355

14. Rao A V, Bhagat S D, Hirashima H, Pajonk G M. Synthesis of flexible silica aerogels using methyltrimethoxysilane (MTMS) precursor. Journal of Colloid and Interface Science, 2006, 300(1): 279–285
15. Luo Y, Li Z, Zhang W, Yan H, Wang Y, Li M, Liu Q. Rapid synthesis and characterization of ambient pressure dried monolithic silica aerogels in ethanol/water co-solvent system. Journal of Non-Crystalline Solids, 2019, 503-504: 214–223
16. Cheng X, Li C, Shi X, Li Z, Gong L, Zhang H. Rapid synthesis of ambient pressure dried monolithic silica aerogels using water as the only solvent. Materials Letters, 2017, 204: 157–160
17. Lana S L B, Seddon A B. X-ray diffraction studies of sol-gel derived ORMOSILs based on combinations of tetramethoxysilane and trimethoxysilane. Journal of Sol-Gel Science and Technology, 1998, 13(1): 461–466
18. Widati A A, Nuryono N, Kartini I. Water-repellent glass coated with SiO_2-TiO_2-methyltrimethoxysilane through sol-gel coating. AIMS Materials Science, 2019, 6(1): 10–24
19. Moriones P, Echeverria J C, Parra J B, Garrido J J. Phenyl siloxane hybrid xerogels: structure and porous texture. Adsorption, 2020, 26 (2): 177–188
20. Jeong A Y, Koo S M, Kim D P. Characterization of hydrophobic SiO_2 powders prepared by surface modification on wet gel. Journal of Sol-Gel Science and Technology, 2000, 19(1): 483–487
21. Hering N, Schreiber K, Riedel R, Lichtenberger O, Woltersdorf J. Synthesis of polymeric precursors for the formation of nanocrystalline Ti-C-N/amorphous Si-C-N composites. Applied Organometallic Chemistry, 2001, 15(10): 879–886
22. Łączka M, Cholewa-Kowalska K, Kogut M. Organic-inorganic hybrid glasses of selective optical transmission. Journal of Non-Crystalline Solids, 2001, 287(1): 10–14
23. Law K Y. Definitions for hydrophilicity, hydrophobicity, and superhydrophobicity: getting the basics right. Journal of Physical Chemistry Letters, 2014, 5(4): 686–688